Gourlay, T.P. 2008 Dynamic draught of container ships in shallow water. International Journal of Maritime Engineering, Vol 150, Part A4, pp 43 – 56.

DYNAMIC DRAUGHT OF CONTAINER SHIPS IN SHALLOW WATER

T.P. Gourlay, Centre for Marine Science and Technology, Curtin University, Western Australia

SUMMARY

Results are presented from a series of full-scale trials to measure the dynamic draught of container ships in shallow water. The measured results are compared with theoretical predictions. The effect of container ship manoeuvring on under-keel clearance is discussed, with particular reference to the increased stern-down trim during turns.

NOMENCLATURE

A_W	Ship waterplane area (m^2)
$B(x)$	Ship waterline beam at station x (m)
c_{s_mid}	Midship sinkage coefficient (-)
c_{s_LCF}	LCF sinkage coefficient (-)
c_θ	Trim coefficient (-)
F_h	Depth-based Froude number (-)
g	Acceleration due to gravity ($m\ s^{-2}$)
θ	Stern-down change in trim due to squat (m)
h	Water depth (m)
I_W	Second moment of waterplane area (m^4)
k	Fourier wave number (m^{-1})
L	Ship submerged length (m)
L_{OA}	Ship length overall (m)
L_{PP}	Ship length between perpendiculars (m)
s_{aft}	Sinkage at aft perpendicular (m)
s_{fwd}	Sinkage at forward perpendicular (m)
s_{LCF}	Sinkage at LCF (m)
s_{mid}	Sinkage at midships (m)
$S(x)$	Ship section area at station x (m)
T_{aft}	Draught at aft perpendicular (m)
T_{fwd}	Draught at forward perpendicular (m)
U	Ship speed through water ($m\ s^{-1}$)
∇	Ship volume displacement (m^3)
x	Longitudinal coordinate (m)
x_{LCF}	Position of longitudinal centre of floatation (m)
x_{mid}	Position of midships (m)

1. INTRODUCTION

In February 2005, a set of 20 full-scale trials was undertaken on 16 deep-draught container ships entering or leaving Hong Kong harbour (Kwai Chung) via the Western Fairway. The transit was effectively in calm water, with only small, short period waves present. The trials procedure and general dynamic draught calculations were described in Gourlay & Klaka (2007).

In the trials, measurements were made of the vertical elevation of three points on each ship, using real-time kinematic GPS receivers measuring at 1 second intervals. By comparing the dynamic readings to stationary readings taken at the berth, the change in vertical position of the ship when under way (relative to the static position) could be determined. Corrections were made for the changing tide height and geoid undulation.

Figure 1 shows the concept of dynamic sinkage and dynamic trim, as measured during the trials. The ship sinks down relative to the still water level when under way, due to its forward movement and environmental effects. Neglecting heel for the moment, the dynamic sinkage is characterized by a dynamic sinkage s_{fwd} at the forward perpendicular, and dynamic sinkage s_{aft} at the aft perpendicular. The midship sinkage is then $(s_{aft} + s_{fwd})/2$. The static trim is $(T_{aft} - T_{fwd})$, while the dynamic trim is $(s_{aft} - s_{fwd})$.

By measuring the vertical position of three points on the ship, and assuming the ship to be rigid, the vertical elevation results were used to calculate midship sinkage, dynamic trim and dynamic heel. Dynamic heel is here defined as the change in heel angle relative to the static floating position.

In practice, dynamic sinkage has steady and unsteady components. A steady midship sinkage and dynamic trim occur due to constant forward speed in constant water depth (commonly called “squat”). A steady breeze or a steady rate of turn can produce a steady heel angle. However, many unsteady effects on dynamic sinkage occur over varying time scales. Wave action, ship acceleration, depth changes, rudder movement and wind gusts all produce “unsteady” effects on dynamic sinkage, which can be difficult to separate from the “steady” effects.

For this reason, we shall leave the “steady” and “unsteady” components of vertical movement together, and make the following definitions for the purposes of this article:

1. “Midship sinkage” is the total downward displacement of the ship’s midships on the centreline, relative to the static floating position, at any instant in time. This includes the short-period midship oscillations commonly called “heave”.
2. “Dynamic trim” is the ship’s total change in trim (positive stern-down), relative to the static floating position, at any instant in time. This includes the short-period oscillations commonly called “pitch”.
3. “Dynamic heel” is the ship’s total change in heel (positive to starboard), relative to the static floating position, at any instant in time. This includes the short-period oscillations commonly called “roll”.

With these definitions, the dynamic sinkage of any point on the ship, relative to the still water level, is completely described by its midship sinkage, dynamic trim and dynamic heel at that instant. Adding the dynamic sinkage at each point on the ship to its static draught at that point, the dynamic draught at each point on the ship can be found, as described in Gourlay & Klaka (2007). The point on the hull with the largest dynamic draught is the part of the hull that is closest to the seabed at that instant, if the seabed is locally flat and horizontal. Therefore the overall dynamic draught, which is the largest value over all of the hull extremities, governs the net under-keel clearance and hence grounding risk. If the seabed is rocky or irregular, the point on the hull most likely to ground may not be the point with the largest dynamic draught. However in this case a conservative underkeel clearance calculation should use the minimum water depth in the area, combined with the dynamic draught as described above.

In this article we shall look in detail at the components of dynamic draught, and compare the individual components with theoretical predictions.

2. THEORETICAL MIDSHIP SINKAGE AND DYNAMIC TRIM PREDICTIONS

2.1 TUCK METHOD

The theoretical method used to compare against the measured midship sinkage and dynamic trim results is the Tuck (1966) method, modified slightly to cater to ships with transom sterns, as in Gourlay (2008). According to this method, the sinkage at the longitudinal centre of floatation (LCF), or at midships (midway between forward and aft perpendiculars), can be written

$$s_{\mathrm{LCF}} = c_{\mathrm{s\_LCF}} \frac{\nabla}{L_{\mathrm{PP}}^2} \frac{F_h^2}{\sqrt{1-F_h^2}} \tag{1}$$

$$s_{\mathrm{mid}} = c_{\mathrm{s\_mid}} \frac{\nabla}{L_{\mathrm{PP}}^2} \frac{F_h^2}{\sqrt{1-F_h^2}} \tag{2}$$

where

$$F_h = \frac{U}{\sqrt{gh}} = \text{depth-based Froude number} \tag{3}$$

Similarly, the stern-down change in trim due to squat θ, which is the stern (aft perpendicular) sinkage minus bow (forward perpendicular) sinkage, can be written

$$\theta = c_\theta \frac{\nabla}{L_{\mathrm{PP}}^2} \frac{F_h^2}{\sqrt{1-F_h^2}} \tag{4}$$

The coefficients $c_{\mathrm{s\_LCF}}$ and c_θ are calculated in terms of the waterline beam distribution $B(x)$ and section area distribution $S(x)$. The longitudinal coordinate x is defined such that $x = 0$ at the forward extremity of the submerged hull, and $x = L$ at the aft extremity of the submerged hull. The first step is to calculate the Fourier transforms

$$\overline{S'}(k) = \int_0^L S'(x)\, e^{ikx} dx \tag{5}$$

$$\overline{B^*}(k) = \int_0^L B(x)\, e^{-ikx} dx \tag{6}$$

$$\overline{xB^*}(k) = \int_0^L (x - x_{\mathrm{LCF}})\, B(x)\, e^{-ikx} dx \tag{7}$$

Here $S'(x)$ is the derivative of the ship's section area with respect to x, and is used so as to allow transom sterns as described in Gourlay (2008). The waterplane area and second moment of area are also calculated:

$$A_{\mathrm{W}} = \int_0^L B(x)\, dx \tag{8}$$

$$I_{\mathrm{W}} = \int_0^L (x - x_{\mathrm{LCF}})^2\, B(x)\, dx \tag{9}$$

The LCF sinkage and trim coefficients are then given as follows:

$$c_{\mathrm{s\_LCF}} = \frac{L_{\mathrm{PP}}^2}{4\pi A_{\mathrm{W}} \nabla} \int_{-\infty}^{\infty} i\, \overline{S'}(k)\, \overline{B^*}(k) \mathrm{sgn}(k)\, dk \tag{10}$$

$$c_\theta = \frac{L_{\mathrm{PP}}^3}{4\pi I_{\mathrm{W}} \nabla} \int_{-\infty}^{\infty} i\, \overline{S'}(k)\, \overline{xB^*}(k) \mathrm{sgn}(k)\, dk \tag{11}$$

The sign function is

$$\mathrm{sgn}(k) = \begin{cases} -1 & k < 0 \\ 0 & k = 0 \\ 1 & k > 0 \end{cases} \tag{12}$$

Assuming a near-rigid hull, the LCF sinkage and midship sinkage are related geometrically through

$$s_{\mathrm{mid}} = s_{\mathrm{LCF}} + \frac{(x_{\mathrm{mid}} - x_{\mathrm{LCF}})\theta}{L_{\mathrm{PP}}} \tag{13}$$

Hence $c_{\mathrm{s\_mid}}$ can be determined from

$$c_{\mathrm{s\_mid}} = c_{\mathrm{s\_LCF}} + \frac{(x_{\mathrm{mid}} - x_{\mathrm{LCF}}) c_\theta}{L_{\mathrm{PP}}} \tag{14}$$

The sinkage and trim coefficients are non-dimensional, and are unaffected by stretching of the ship in any direction. The midship sinkage coefficient $c_{\mathrm{s\_mid}}$ is nearly constant for most ships, varying from 1.2 to 1.5 over a wide range of container ship and bulk carrier hull forms. The trim coefficient c_θ is sensitive to the longitudinal section area and waterline beam distribution, which can be partly described by the LCB (longitudinal centre of buoyancy) and LCF. For example, bulk carriers with their LCB well forward of the LCF tend to have negative c_θ and hence bow-down dynamic trim. Container ships, with the LCB closer to the LCF, may have either bow-down or stern-down dynamic trim, as

predicted by the theory and evidenced by the trials described here.

2.2 QUASI-STEADY APPROXIMATION

The theoretical method described above was developed for constant ship speed, in open water of constant depth. However for slowly-varying ship speed and/or water depth, the theory can be used as a quasi-steady theory, by applying the ship speed and water depth at any instant through the transit. Full unsteady versions of the same method do exist (see e.g. Plotkin 1976, Gourlay 2003), but are limited to simple depth profiles and hull shapes.

2.3 INPUTS

The required inputs for the theoretical predictions were determined as follows.

Ship hull shape
Without having access to exact hull offsets, the hull can be modelled by starting with a typical container ship hull and modifying it to match the main hull parameters of the hull in question. These parameters can be found from the stability booklet at the appropriate midship draught and trim.

Ship speed through water
Ship speed over ground is a direct output from the GPS measured data. The tide gauges near the Western Fairway do not measure stream speed, so speed through water could not be determined from the speed over ground and stream speed. However it was estimated that stream speeds were less than 0.5 knots for all of the measured transits, with ship speeds in the area of interest generally between 8 and 13 knots. Therefore using speed over ground may have produced around a 5% error in estimating speed through water. At depth-based Froude numbers up to 0.4 or 0.5, as in these trials, a 5% speed through water error would produce a 10% error in the predicted sinkage and trim.

An alternative method to determine speed through water is to use the readings from the ship's doppler or impeller log. However, these generally only give a visual display, so obtaining an accurate time-stamped record of the speed through water was not feasible. Also, the logs have appreciable error in shallow water. Therefore, given the weak tidal streams, using speed over ground to estimate speed through water was seen as the most accurate method, and this is the method that has been used.

Water depth profile
Chart datum depths have been found by digitizing a nautical chart of the Western Fairway, extending from the Kwai Chung container terminals in the north, to the southern extent of the measurement area at 22º16.5´N. The measurement area covered a transit length of around 3.5 nautical miles, mainly in a north-south direction. The digitized chart datum depths have been interpolated to map the entire area. Note that since the charted depths correspond to the shallowest water depth in each location, the interpolated depths will tend to underestimate the water depths slightly.

The transit is essentially "open-water" as far as squat models are concerned, with no significant depth variations transverse to the ships' track, other than an area of shallower water on the eastern side, and islands further to the east. As discussed, longitudinal depth variations are catered for by assuming quasi-steady flow; the errors inherent in this will be discussed subsequently.

Tidal heights were measured at Kwai Chung and surrounding tide gauges for each transit. These were used to determine tide height through each transit, as described in Gourlay & Klaka (2007). Tide heights were added to the chart datum depths, to obtain the total water depth as a function of space and time.

3. THEORETICAL DYNAMIC HEEL PREDICTIONS

The theoretical dynamic heel due to wind was calculated using the IMO (2005) method, while the dynamic heel due to turning was calculated using the steady-state formula given in Clark (2005). The input parameters required are:

- wind speed and direction
- ship heading and rate of turn
- ship profile area and centroid height
- ship centre of gravity height and transverse metacentric height

These inputs were determined as follows.

Wind speed and direction
Mean wind speed and direction were measured at Green Island, which is adjacent to the Western Fairway in the measurement area, and lies in clear air for the prevailing ENE winds in February.

Ship heading and rate of turn
Ship heading is calculated from the ship GPS measurements, by calculating the GPS position of the bow and bridge centreline at each sample. The ship heading is differentiated to find the instantaneous rate of turn. The ship heading is combined with the wind speed and direction to find the beam wind component.

Ship profile area and centroid height
Since exact data were not available, the profile area and centroid height were approximated by assuming a rectangular profile with length equal to the ship's length between perpendiculars, and height above the waterline equal to 20 metres.

Ship centre of gravity height and transverse metacentric height
This information was obtained from the ship's loading calculations and stability booklet.

4. SHIPS ANALYZED

The ships chosen for analysis are those for which the required hull information was available, so that theoretical predictions could be calculated. The ships for which sinkage and trim results are given, together with their relevant dimensions, are shown in Table 1.

The ships for which dynamic heel results are given, together with their relevant details, are shown in Table 2.

5. RESULTS

5.1 MIDSHIP SINKAGE

The midship sinkage coefficient for each ship, as calculated from equation (14), is shown in Table 3. The theoretical sinkage at each instant through the transit is then calculated using equation (2).

Measured and predicted midship sinkage for the three example transits, together with measured speed over ground and calculated water depth, are shown in Figures 2 to 4.

The measured sinkage is unfiltered. As discussed in Gourlay & Klaka (2007), the expected RMS error in absolute midship sinkage is around 0.05m, mostly due to uncertainty in the static reading. The short-period random GPS error is around 0.01 to 0.02m. We notice from the graphs that the oscillation amplitudes are typically around 0.02 to 0.03m, so the random GPS errors may make up a significant portion of this. However, a Fourier analysis on the midship sinkage oscillations found that the principal oscillation component was in each case close to the estimated natural heave period in shallow water (around 9 seconds for Katrine Maersk, and 8.5 seconds for Sally and Sofie Maersk). These heave oscillations may be caused by unsteady effects such as changes in depth, speed or acceleration. In addition, there was negligible energy at short periods (<5s). Therefore it appears likely that the measured midship sinkage oscillations are predominantly due to actual heave, and any filtering of the data would remove this real effect. Therefore the results were left in raw form, on the understanding that they contain a short-period random GPS error of around 0.01 to 0.02m, and absolute RMS error of around 0.05m.

The measured results show the effect of speed and water depth on midship sinkage. The ship speed generally increases toward the southern end of the transit, while the channel is comparatively deep around 22º18.5´N, and comparatively shallow around 22º17.5´N. The combined effects of speed and depth result in a midship sinkage that generally increases toward the southern end of the transit (due to increasing speed), but with the midship sinkage being smaller near 22º18.5´N (due to increased depth) and larger near 22º17´N (due to decreased depth).

Given that each transit involves significant speed changes and depth changes, the overall performance of the theoretical method is quite good. However, there are some important differences, which serve to highlight the importance of unsteady effects on ship squat.

For the outbound ships (heading south), it can be seen that Sofie Maersk's midship squat is approximately as predicted, while Sally Maersk shows more oscillatory behaviour between 22º18´N and 22º17´N. By comparing the speed and water depth profiles for each transit, we see that Sally Maersk experiences larger acceleration over this period, and also a more abrupt depth change, being further east in the channel. Both of these factors decrease the validity of the "quasi-steady" assumption, resulting in significant vertical accelerations and hence oscillatory motions.

For Katrine Maersk inbound, a large departure from the predicted midship sinkage occurs around 22º17.5´N. Being on the eastern side of the channel, she experiences relatively rapid depth shoaling, at the same time as she is decelerating. The combined effect appears to be a significant decrease in midship sinkage, as compared to the quasi-steady prediction.

Also worthy of note for Katrine Maersk is the under-prediction of midship squat around 22º19´N. At that time, she is on the eastern side of the channel, travelling parallel to a 9m shoal. As described in Beck et al (1975), this "dredged channel" configuration tends to increase the midship squat, as compared to the open-water case.

5.2 DYNAMIC TRIM

The theoretical trim coefficient for each ship, as calculated using equation (9), is shown in Table 3. Because the trim coefficient is quite sensitive to the hull shape, and the modelled hull forms are only approximate, the trim coefficients should also be considered approximate.

All three cases considered here involved positive trim coefficient, giving a positive (stern-down) dynamic trim. This is due to the fine lines of the K and S Class ships, with LCB slightly aft of midships. It should be noted that some of the higher block-coefficient container ships, with LCB further forward, were seen to have a negative dynamic trim.

Katrine Maersk, having the largest draught, has the smallest trim coefficient. This is partly due to the LCF moving farther aft as the draught increases.

Measured and predicted dynamic trim for the three example transits are shown in Figures 5 to 7.

Again, the measured dynamic trim is unfiltered. Following Gourlay & Klaka (2007), since trim is based on the difference between bow and bridge measurements, interpolated to the forward and aft perpendiculars, the

expected RMS error in absolute dynamic trim is around 0.07m, mostly due to uncertainty in the static reading. The short-period random GPS error is around 0.015 to 0.03m. We notice from the measured dynamic trim that the oscillation amplitudes are typically around 0.03 to 0.1m, so the random GPS errors may make up a significant portion of the oscillations in some cases. However, a Fourier analysis on the dynamic trim oscillations found that the principal oscillation component was in each case close to the estimated natural pitch period in shallow water (around 10 seconds for Katrine Maersk, and 9 seconds for Sally and Sofie Maersk). Also, as for midship sinkage, there was negligible energy at short periods, so it appears likely that the measured dynamic trim oscillations are predominantly due to actual pitching. Therefore the results have been left in raw form, with an associated short-period random GPS error of around 0.015 to 0.03m, and absolute RMS error of around 0.07m.

The measured dynamic trim is generally positive (stern-down) for Sofie and Sally Maersk, and generally positive but sometimes negative for Katrine Maersk.

For Sofie and Sally Maersk, the measured dynamic trim generally follows the theoretical predictions, increasing as the speed increases and decreasing as the depth increases, just as the midship sinkage does. For Sally Maersk, the oscillatory effects that are noted in the midship sinkage are also evident in the dynamic trim, with significant oscillations occurring between 22º18´N and 22º17´N.

The effect of acceleration on dynamic trim can be seen for Sofie Maersk. At 22º17´N she stops accelerating, and her dynamic trim drops at the same time.

For Katrine Maersk inbound, the decrease in midship sinkage at around 22º17.5´N is accompanied by an increased stern-down trim. Therefore the main effect of the combined depth shoaling and deceleration is a significant decrease in bow sinkage.

If we study the dynamic trim plots, we notice that some large changes in dynamic trim occur in regions of near-constant speed and water depth. The cause of these changes is the ship's rate of turn, which will be discussed subsequently.

5.3 DYNAMIC HEEL

Measured and predicted dynamic heel for the example transits are shown in Figures 8 to 10. As for sinkage and trim, the measured results are unfiltered.

For the transits shown, all turns were toward the east, and the wind was from the ENE. Therefore the predominant heel was to starboard for outbound (southbound) transits, and to port for inbound (northbound) transits.

As described in Section 3, dynamic heel is calculated here using quasi-steady formulae, based on mean wind speed, relative wind direction and instantaneous rate of turn. Therefore the theoretical predictions do not include the following effects, which are seen to be of importance:

Rudder-induced heel
The initial movement of the rudder to commence a turn causes a heeling moment toward the centre of the turn (see e.g. SNAME 1989). Once in the turn, the quasi-steady heeling moment (due to centrifugal forces) is away from the centre of the turn. The combined effect is for the ship to initially heel slightly into the turn, then away from the turn once on a steady arc. The rudder-induced heeling moment is not included in the theoretical predictions. Therefore we can see in all cases that the measured heel "lags" behind the theoretical heel, due to neglect of the rudder-induced heeling moment.

Residual oscillations
The theoretical predictions also do not include the effect of residual heel oscillations following application of the rudder. For the transits shown, it can be seen that the induced heeling moments, due to rudder application and rate of turn, produce residual heel oscillations (roll) that are slowly damped away until the next turning manoeuvre. The measured oscillation periods have been analyzed using Fourier transform, and found to approximately coincide with the estimated natural roll periods of 19 seconds for Anna Maersk, 21 seconds for Maersk Dortmund, and 22 seconds for Katrine Maersk.

5.4 EFFECT OF MANOEUVRING ON DYNAMIC TRIM

As mentioned in Section 5.2, some of the measured dynamic trim changes could not be explained with reference to changes in ship speed or water depth. As well as these factors, rate of turn was also seen to have an important effect on dynamic trim.

The correlation between stern-down trim and absolute rate of turn, for all of the example transits described, is shown in Figures 11 to 15.

We see that the dynamic trim tends to be more stern-down during turning manoeuvres. The increase in dynamic stern-down trim due to turning was generally around 0.1 to 0.2m, but up to 0.4m for Anna Maersk. Since the rate of turn produced no noticeable effect on midship sinkage, the increase in stern sinkage is half the increase in trim, i.e. 0.05 to 0.1m generally, or up to 0.2m for Anna Maersk. Since the stern was the point on the ship that came closest to the seabed for almost all of the container ship tests (see Gourlay & Klaka 2007), this increase in stern sinkage translates directly into a decrease in net underkeel clearance.

The flow around a hull during a turn is complicated, and it is difficult to attribute the stern-down trim to a single

cause. For example, two important effects of turning are the induced heel angle, and the non-symmetric flow around the hull. The *hydrostatic* effect of non-zero heel on container ship trim is generally to trim the ship further by the bow, rather than the stern. Also, the effect of drift angle (such as is experienced during a turn) was studied for container ships in *straight-line* motion (Longo & Stern 2002) and found to also trim the ship further by the bow, rather than the stern. Clearly there is a hydrodynamic effect due to the turning trajectory of the ship which outweighs the basic considerations of heel and drift angle. Measuring and calculating the flow field around a turning ship is a topic which warrants further investigation.

6. CONCLUSIONS

Results have been presented from full-scale GPS trials of container ships entering and leaving Hong Kong harbour. The components of dynamic draught, namely midship sinkage, dynamic trim and dynamic heel, have been analyzed in detail.

Midship sinkage and dynamic trim have been compared with theoretical predictions from the Tuck method. It is seen that the method predicts midship sinkage with reasonable accuracy for moderate speed and depth changes, but that unsteady effects are also important when speed or depth changes are abrupt. The prediction of dynamic trim was more approximate, due to the sensitivity of the theory (and the actual flow) to the longitudinal hull volume distribution. Nevertheless, the general dependence of dynamic trim on speed and water depth was confirmed by the measurements. Like midship sinkage, unsteady effects on dynamic trim were seen to be important when speed or depth changes were abrupt.

The large rate of turn experienced by the ships during this transit gave an opportunity to study dynamic heel, which is an important component of dynamic draught for container ships. Heel angles in the order of 1º to 2º were measured, and the heel angles were reasonably well predicted by the quasi-steady turning and wind formulae.

The turning manoeuvres also allowed identification of an important dynamic draught effect, namely the increased stern-down trim with rate of turn. Since the stern is the point on the hull which normally comes closest to the seabed, this increase in stern-down trim translates into a decrease in under-keel clearance, and should be allowed for accordingly.

7. ACKNOWLEDGEMENTS

The author acknowledges the support of the Hong Kong Marine Department in providing funding and assistance with this research, as well as A.P. Moller - Maersk for providing access to the ships for the measurements, as well as basic hull data. The co-operation of the Hong Kong Pilots' Association in arranging and performing transits is also greatly appreciated.

8. REFERENCES

BECK, R.F., NEWMAN, J.N. & TUCK, E.O., Hydrodynamic forces on ships in dredged channels. *Journal of Ship Research*, Volume 19, No. 3, pp 166 – 171, 1975.

CLARK, I.C., *Ship Dynamics for Mariners*. The Nautical Institute, London, 2005.

GOURLAY, T.P., Slender-body methods for predicting ship squat, *Ocean Engineering*, Volume 35, No. 2, pp 191 – 200, 2008.

GOURLAY, T.P. & KLAKA, K., Full-scale measurements of containership sinkage, trim and roll, *Australian Naval Architect* , Volume 11, No. 2, pp 30 – 36, 2007.

GOURLAY, T.P., Ship squat in water of varying depth, *International Journal of Maritime Engineering*, Volume 145, Part A1, pp 1 – 12, 2003.

INTERNATIONAL MARITIME ORGANIZATION, Revision of the Intact Stability Code, submitted by Japan, *IMO sub-committee on stability and load lines and on fishing vessels' safety*, 48th Session, June 2005.

LONGO, J. & STERN, F., Effects of drift angle on model ship flow, *Experiments in Fluids*, Volume 32, pp 558 – 569, 2002.

PLOTKIN, A. The flow due to a slender ship moving over a wavy wall in shallow water. *Journal of Engineering Mathematics*, Volume 10, No. 3, pp 207 – 218, 1976.

SNAME (Society of Naval Architects and Marine Engineers) *Principles of Naval Architecture*, Volume III, SNAME Publications, 1989.

TUCK, E.O. Shallow water flows past slender bodies. *Journal of Fluid Mechanics*, Volume 26, pp 81 – 95, 1966.

TABLES

	Sofie Maersk	Sally Maersk	Katrine Maersk
Ship particulars			
L_{OA}	347.0m	347.0m	318.2m
L_{PP}	331.5m	331.5m	302.8m
Beam	42.8m	42.8m	42.8m
Summer draught	14.5m	14.5m	14.5m
Transit details			
Transit direction	Outbound	Outbound	Inbound
Draught fwd	11.4m	11.7m	13.2m
Draught aft	12.5m	12.1m	13.2m
Displacement	110,200 tonnes	111,300 tonnes	107,200 tonnes

Table 1: Relevant ship details for sinkage and trim results

	Anna Maersk	Maersk Dortmund	Katrine Maersk
Ship particulars			
L_{OA}	352.3m	294.1m	318.2m
L_{PP}	336.4m	283.0m	302.8m
Beam	42.8m	32.2m	42.8m
Summer draught	15.0m	13.5m	14.5m
Transit details			
Transit direction	Outbound	Inbound	Inbound
Mean wind direction	60º	70º	60º
Mean wind speed	10.1 knots	12.4 knots	15.9 knots
Draught fwd	11.0m	9.2m	13.2m
Draught aft	11.1m	10.7m	13.2m
Displacement	96,600 tonnes	55,000 tonnes (approx.)	107,200 tonnes
KG	15.78m	14.5m (approx.)	17.66m
GM	3.11m	1.45m	2.44m

Table 2: Relevant ship details for dynamic heel results

	Sofie Maersk	Sally Maersk	Katrine Maersk
c_{s_mid}	1.22	1.23	1.30
c_{θ}	0.86	0.78	0.43

Table 3: Theoretical squat coefficients

FIGURES

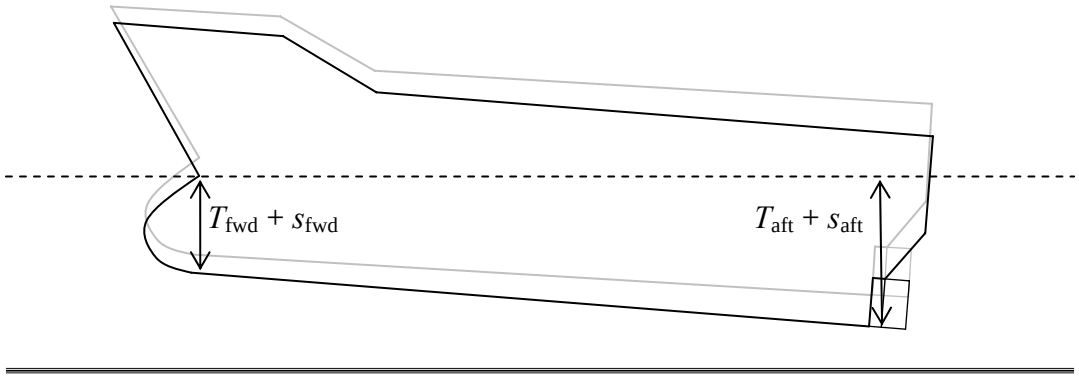

Figure 1: Ship in static floating position (grey outline) and under way (black outline). Dashed line shows undisturbed water level. Ship in static floating position has static draught at forward perpendicular T_{fwd}, and static draught at aft perpendicular T_{aft}. Ship under way has dynamic sinkage at forward perpendicular s_{fwd}, and dynamic sinkage at aft perpendicular s_{aft}.

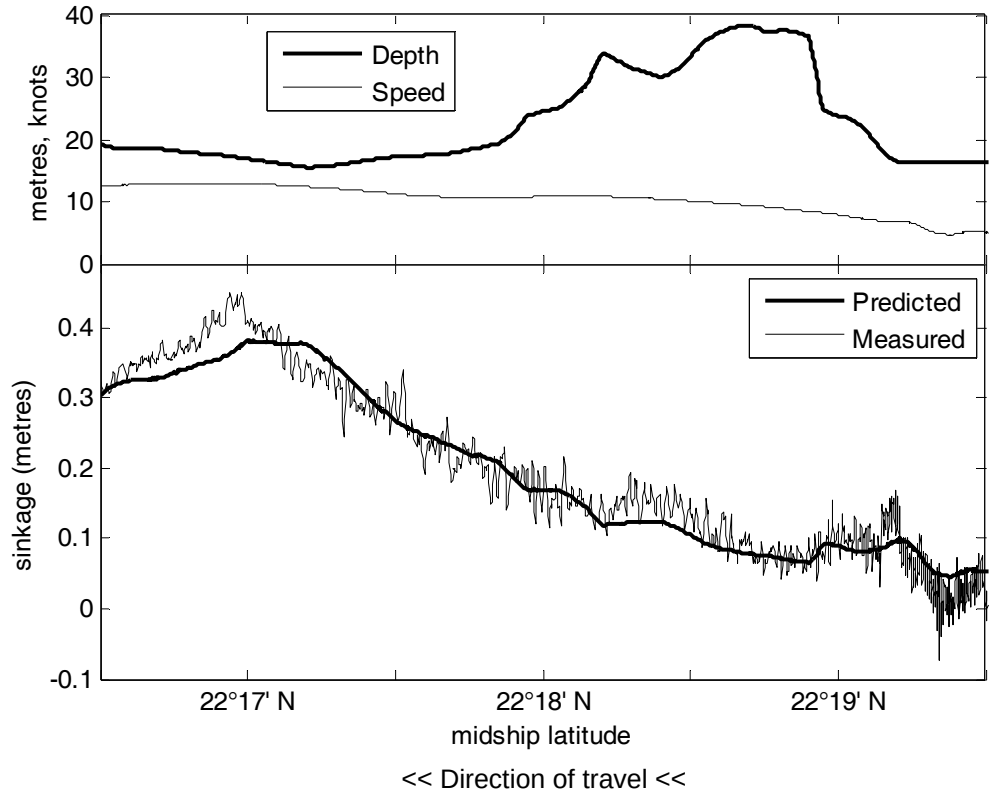

Figure 2: Measured and predicted midship sinkage (positive downward) for Sofie Maersk outbound. Corresponding water depth at midships and speed over ground also shown.

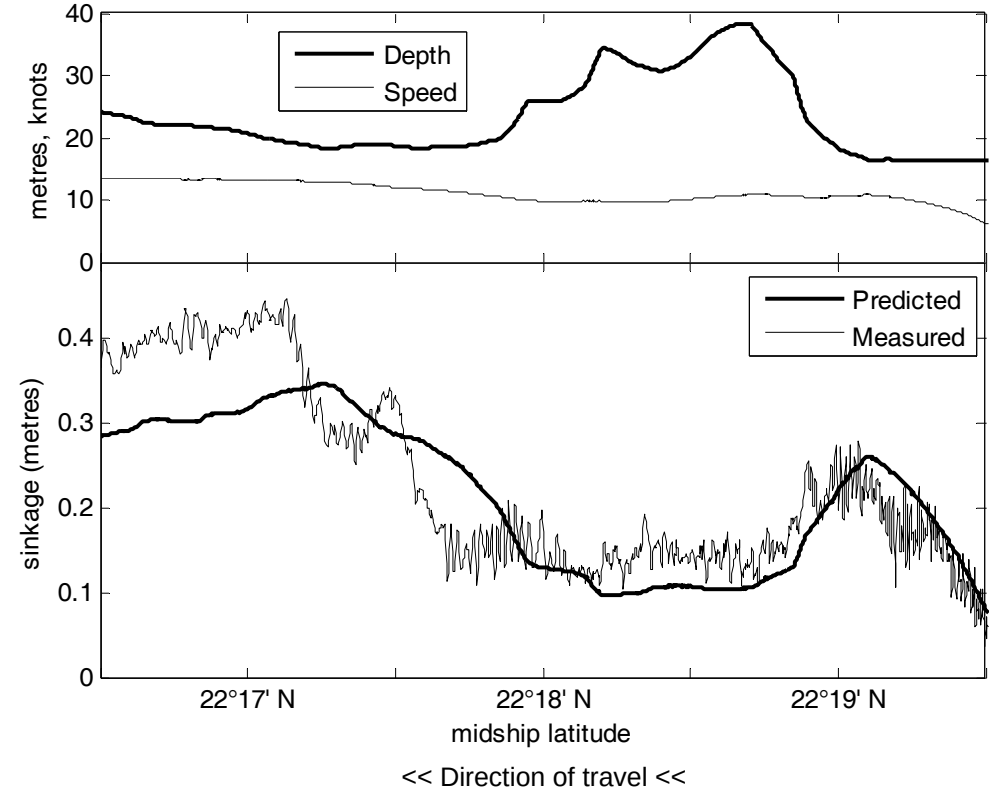

Figure 3: Measured and predicted midship sinkage (positive downward) for Sally Maersk outbound. Corresponding water depth at midships and speed over ground also shown.

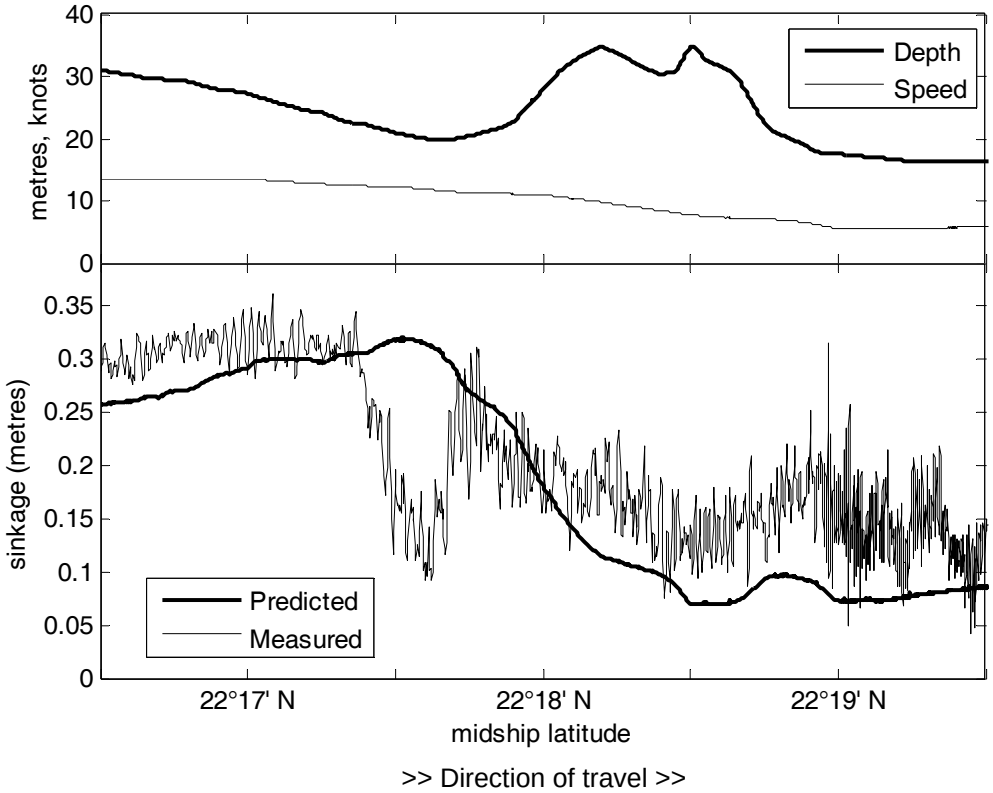

Figure 4: Measured and predicted midship sinkage (positive downward) for Katrine Maersk inbound. Corresponding water depth at midships and speed over ground also shown.

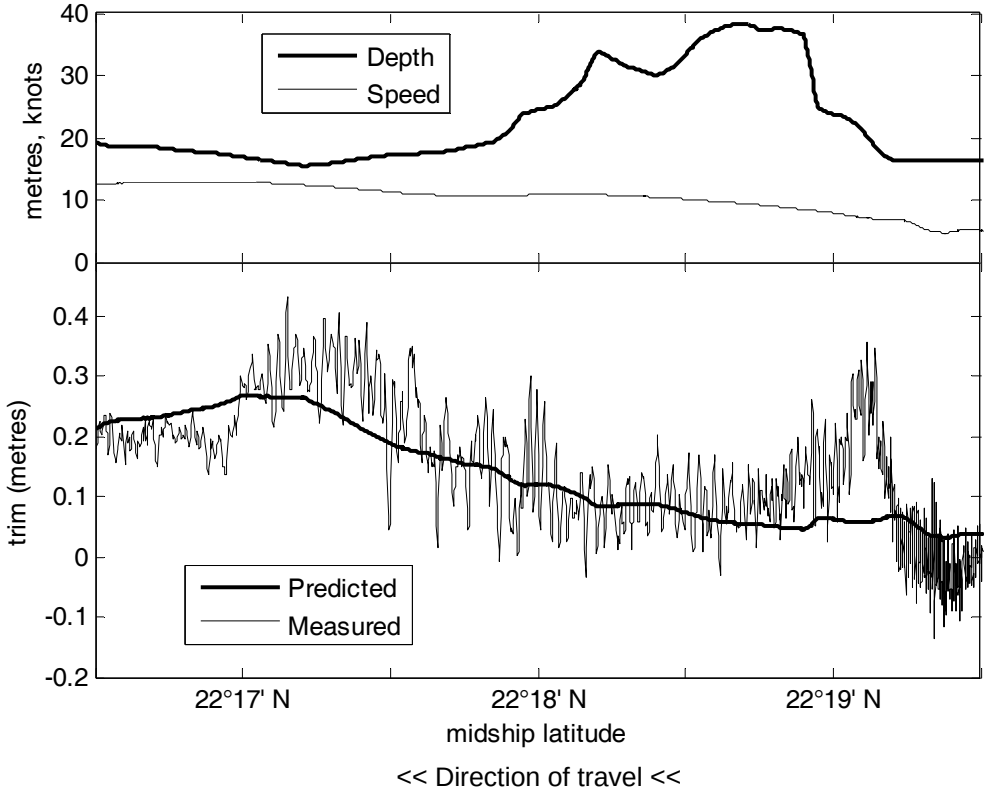

Figure 5: Measured and predicted dynamic trim (positive stern-down) for Sofie Maersk outbound. Corresponding water depth at midships and speed over ground also shown.

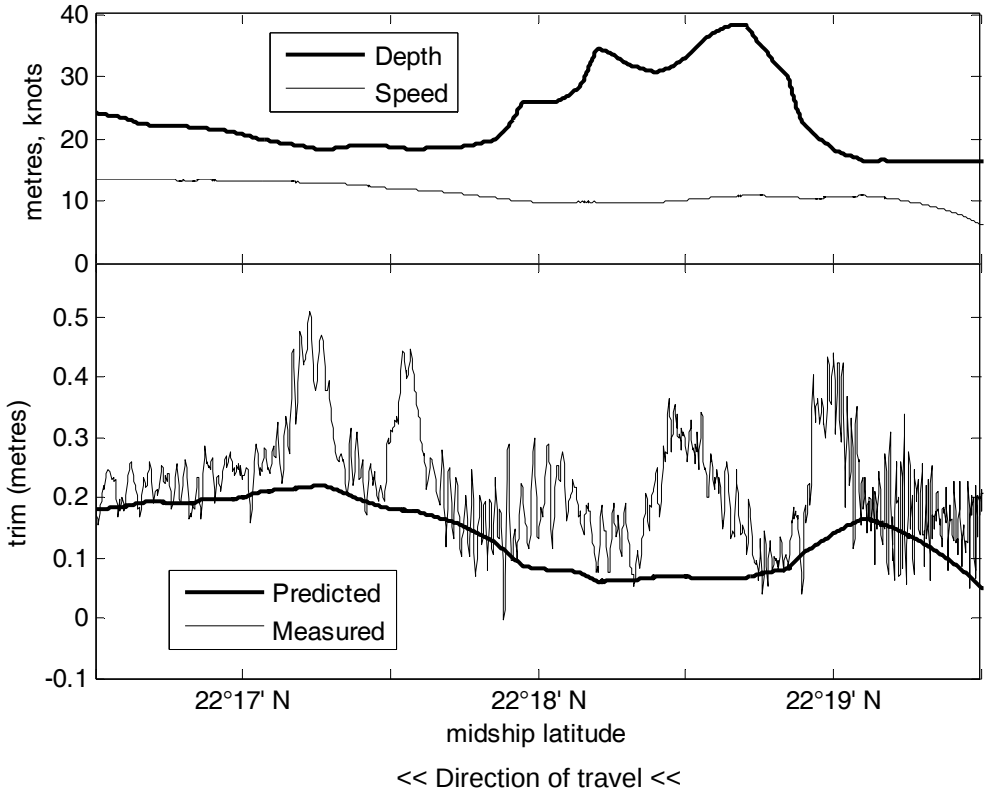

Figure 6: Measured and predicted dynamic trim (positive stern-down) for Sally Maersk outbound. Corresponding water depth at midships and speed over ground also shown.

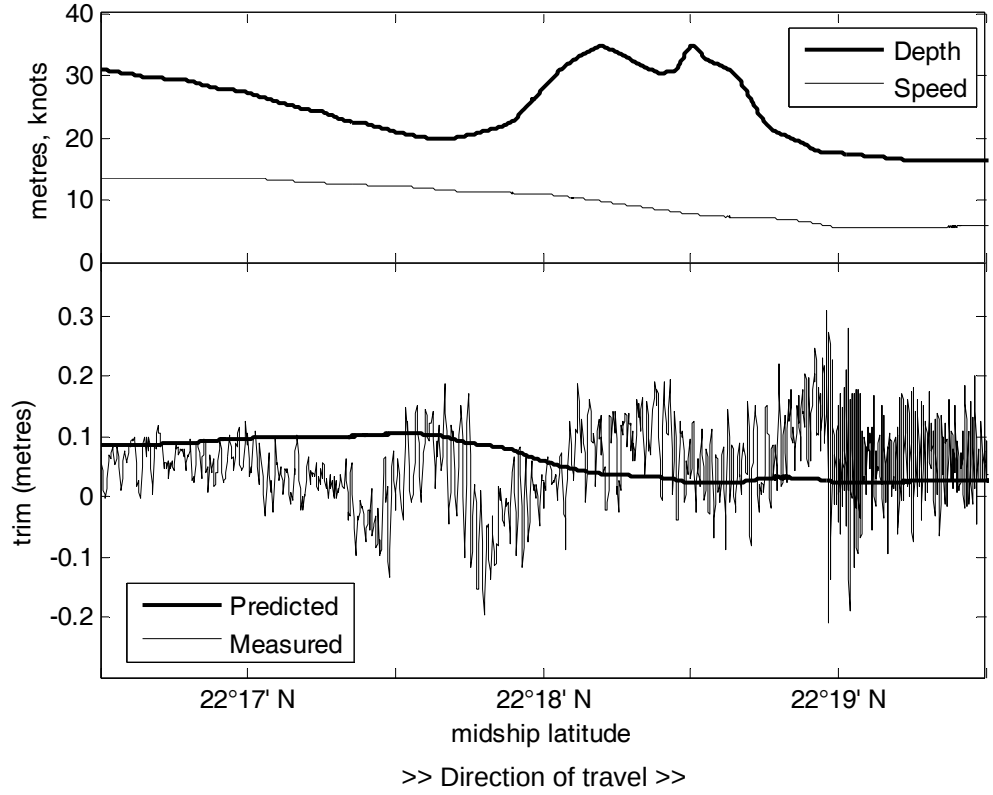

Figure 7: Measured and predicted dynamic trim (positive stern-down) for Katrine Maersk inbound. Corresponding water depth at midships and speed over ground also shown.

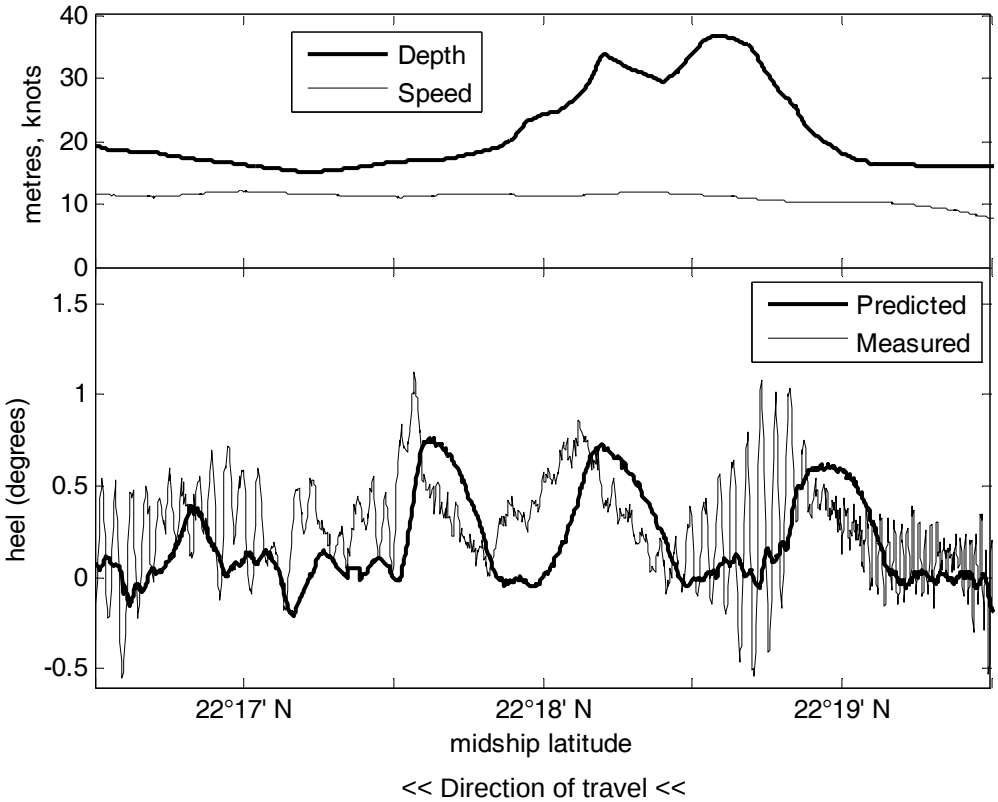

Figure 8: Measured and predicted dynamic heel (positive to starboard) for Anna Maersk outbound. Corresponding water depth at midships and speed over ground also shown.

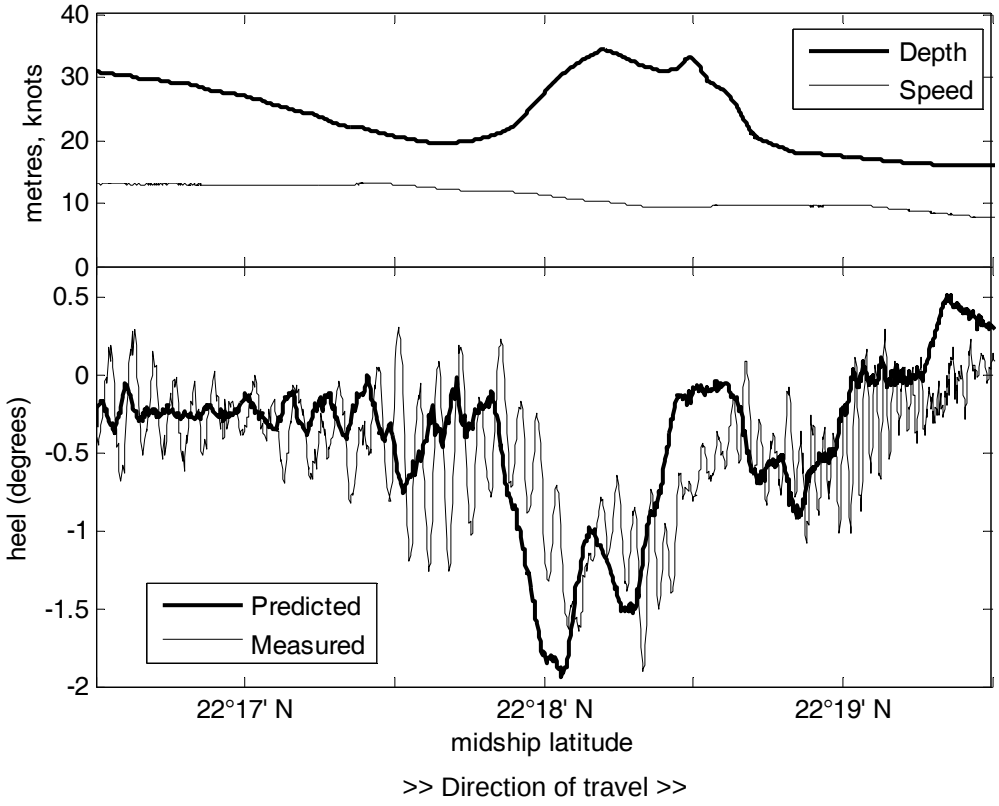

Figure 9: Measured and predicted dynamic heel (positive to starboard) for Maersk Dortmund inbound. Corresponding water depth at midships and speed over ground also shown.

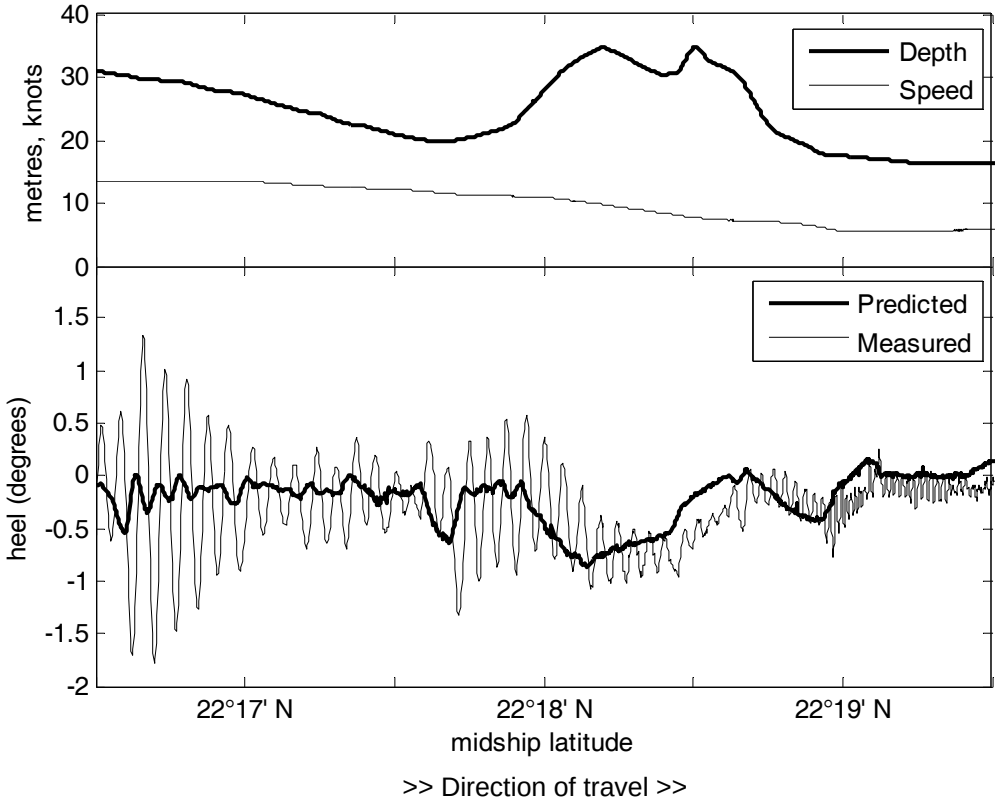

Figure 10: Measured and predicted dynamic heel (positive to starboard) for Katrine Maersk inbound. Corresponding water depth at midships and speed over ground also shown.

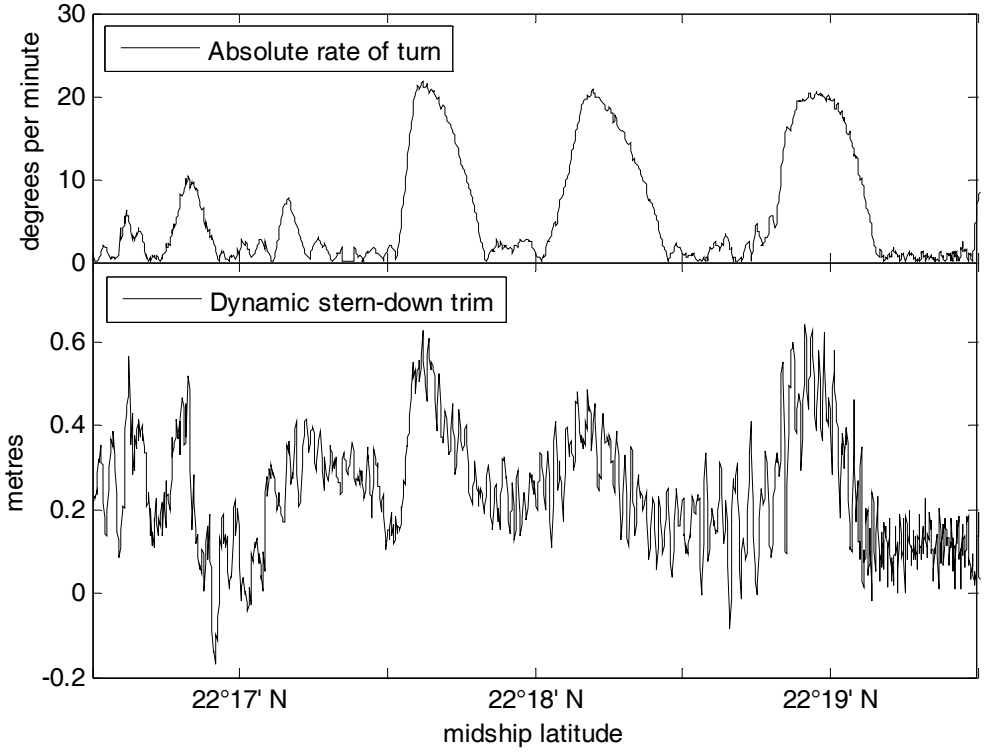

Figure 11: Correlation between rate of turn and dynamic trim for Anna Maersk outbound

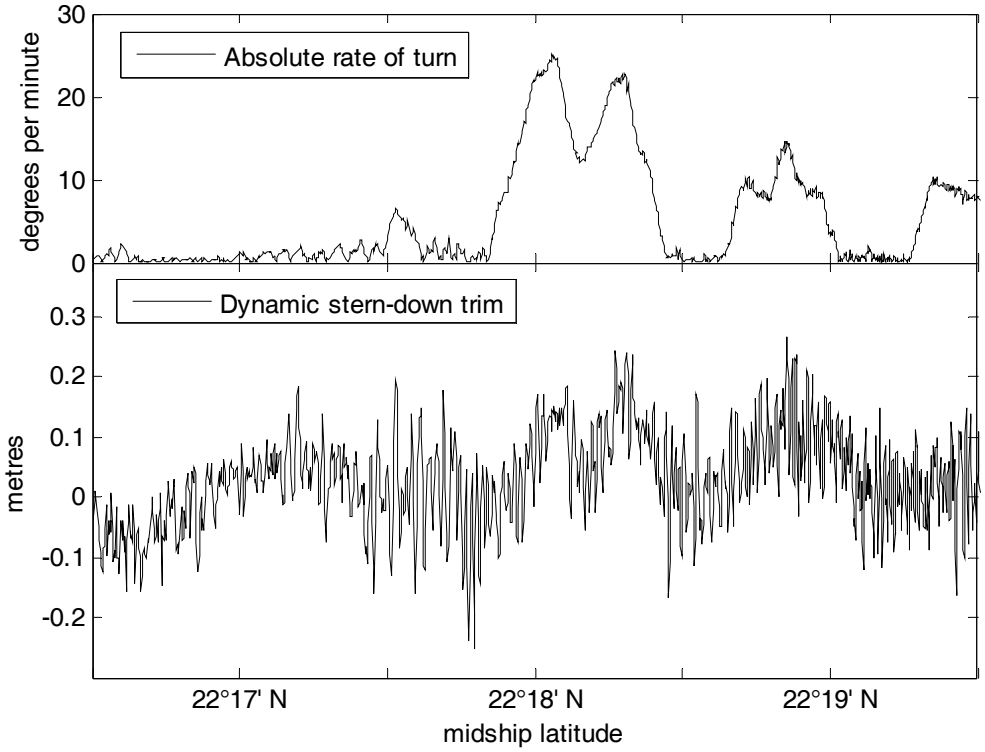

Figure 12: Correlation between rate of turn and dynamic trim for Maersk Dortmund inbound

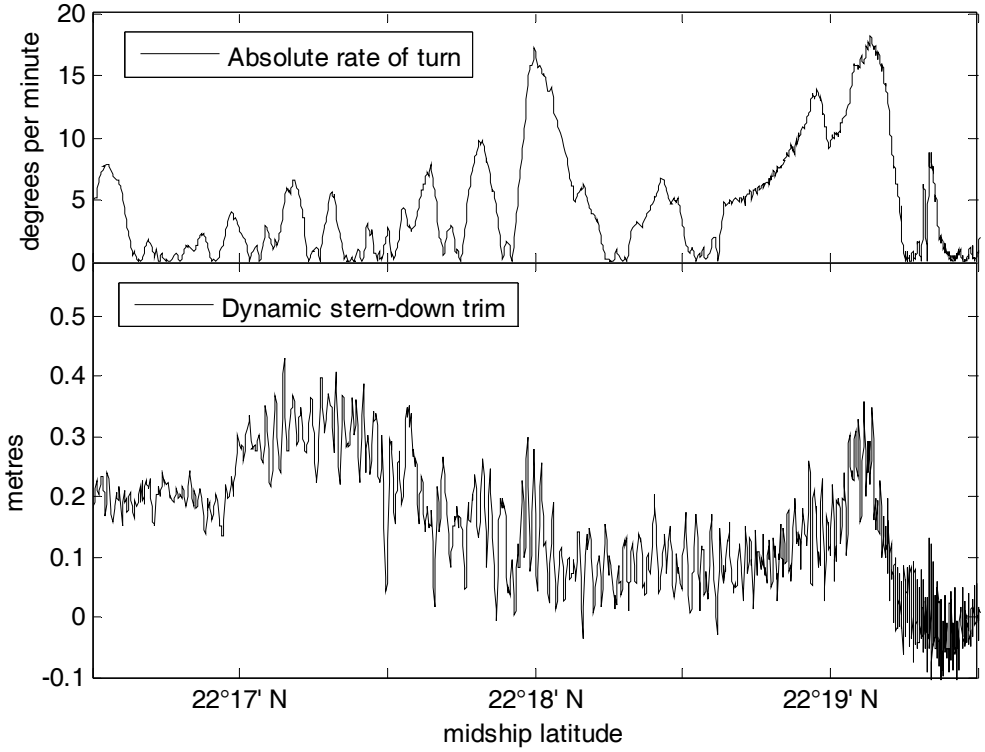

Figure 13: Correlation between rate of turn and dynamic trim for Sofie Maersk outbound

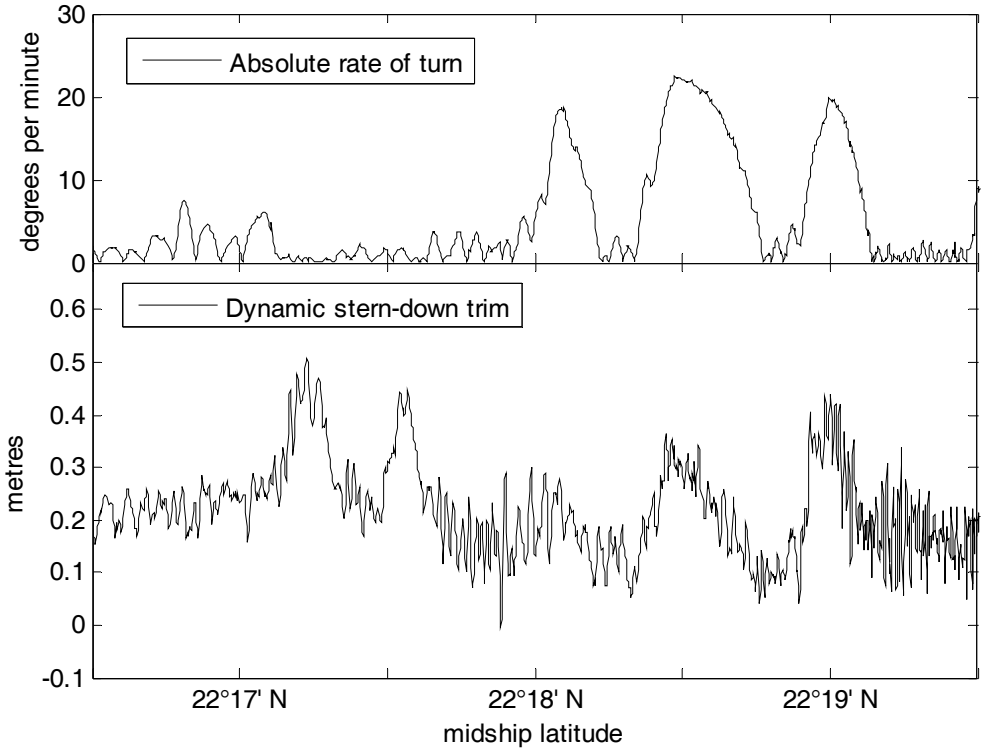

Figure 14: Correlation between rate of turn and dynamic trim for Sally Maersk outbound

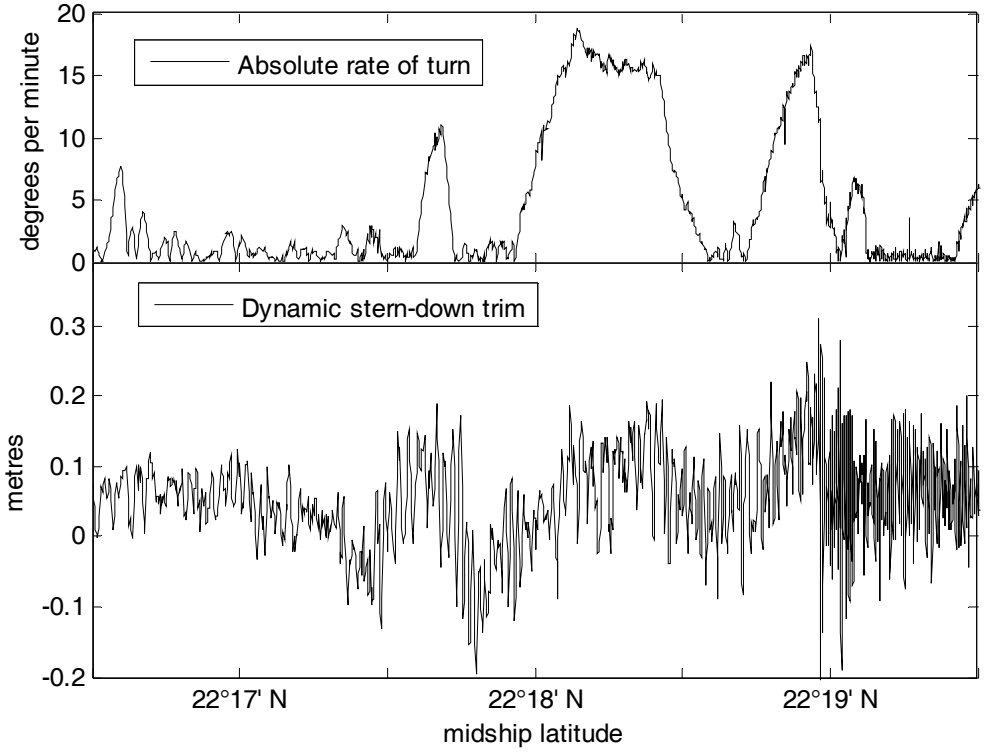

Figure 15: Correlation between rate of turn and dynamic trim for Katrine Maersk inbound